Genetic modifiers regulating DNA replication and double strand break repair are associated with differences in mammary tumors in mouse models of Li-Fraumeni Syndrome

Prabin Dhangada Majhi[1,2], **Nicholas B. Griner**[1], **Jacob A. Mayfield**[3], **Shannon Compton**[1], **Jeffrey J. Kane**[4], **Trevor A. Baptiste**[1], **Karen A. Dunphy**[1], **Amy L. Roberts**[1], **Sallie S. Schneider**[5,6], **Evan M. Savage**[7], **Divyen Patel**[7], **Anneke C. Blackburn**[8], **Kim Joana Maurus**[9], **Lisa Wiesmüller**[9], **D. Joseph Jerry**[1,6]

[1]Department of Veterinary & Animal Sciences, University of Massachusetts Amherst, MA, USA

[2]Department of Botany, Ravenshaw University, Cuttack, Odisha, India

[3]Division of Rheumatology, Inflammation, and Immunity, Brigham and Women's Hospital, Boston, MA, USA

[4]Department of Microbiology, University of Massachusetts Amherst, MA, USA

[5]Department of Surgery, University of Massachusetts Medical School/Baystate, Springfield, MA 01199, USA

[6]Pioneer Valley Life Sciences Institute, Springfield, MA, USA

[7]Genome Explorations, 1910 Nonconnah Blvd #120, Memphis, TN 38132 USA

[8]John Curtin School of Medical Research, Australian National University, Canberra, ACT, Australia

[9]Department of Obstetrics and Gynecology, Ulm University, Ulm, Germany

Abstract

Breast cancer is the most common tumor among women with inherited variants in the *TP53* tumor suppressor, but onset varies widely suggesting interactions with genetic or environmental factors. Rodent models haploinsufficient for *Trp53* also develop a wide variety of malignancies associated with Li-Fraumeni Syndrome, but BALB/c mice are uniquely susceptible to mammary tumors and is genetically linked to the *Suprmam1* locus on chromosome 7. To define mechanisms that interact with deficiencies in p53 to alter susceptibility to mammary tumors, we fine-mapped the *Suprmam1* locus in females from an N2 backcross of BALB/cMed and C57BL/6J mice. A major modifier was localized within a 10 cM interval on chromosome 7. The effect of the locus on DNA damage responses was examined in the parental strains and mice that are congenic for C57BL/6J alleles on the BALB/cMed background (SM1-*Trp53*$^{+/-}$). The mammary epithelium of C57BL/6J-

Corresponding Authors: D. Joseph Jerry, jjerry@vasci.umass.edu; Tel: 413-545-5335; Lisa Wiesmüller, lisa.wiesmueller@uni-ulm.de; Tel: +49-(0)731-500 58800.

The authors declare no potential conflicts of interest.

Trp53$^{+/−}$ females exhibited little radiation-induced apoptosis compared to BALB/cMed-*Trp53*$^{+/−}$ and SM1-*Trp53*$^{+/−}$ females indicating that the *Suprmam1*$^{B6/B6}$ alleles could not rescue repair of radiation-induced DNA double-strand breaks mostly relying on non-homologous end joining. In contrast, the *Suprmam1*$^{B6/B6}$ alleles in SM1-*Trp53*+/− mice were sufficient to confer the C57BL/6J-*Trp53*$^{+/−}$ phenotypes in homology-directed repair and replication fork progression. The *Suprmam1*$^{B6/B6}$ alleles in SM1-*Trp53*$^{+/−}$ mice appear to act in trans to regulate a panel of DNA repair and replication genes which lie outside the locus.

Significance: Genetic variation in replication-associated DNA repair can modify consequences of heterozygous mutations in *Trp53* and contribute to susceptibility to mammary tumors in mouse models of Li-Fraumeni syndrome.

Keywords

Breast cancer; Li-Fraumeni syndrome; *TP53*; Genetic modifiers; Genetic mapping; DNA repair; Replication-associated repair

---

Introduction

The critical role of the p53 protein in suppression of carcinogenesis is reflected by cancer susceptibility among individuals with inherited mutations in the *TP53* gene and its frequent mutation in nearly all types of cancer; however, the tissues affected and the age at which cancers are diagnosed varies dramatically among individuals even when inheriting the same mutations [1]. The overall penetrance of cancer among carriers of established pathogenic variants associated with Li-Fraumeni Syndrome (LFS) is 58% by age 50 and 80% by age 70 [2]. The varied phenotypes suggest that environmental exposures and genetic polymorphisms in other genes play significant roles in modifying the consequences of mutations in *TP53* and the risk of cancer.

Breast cancer is, by far, the most common tumor among women inheriting pathogenic variants in *TP53* [2] indicating the reliance on the p53 pathway in breast epithelial cells. Multi-gene panel testing of women with breast cancer has demonstrated that germline pathogenic variants of *TP53* are far more frequent than previously recognized and often lack the strict familial clustering [3]. Breast cancer is recognized as a polygenic disease and genome-wide association studies (GWAS) have identified >180 variants affecting risk of breast cancer [4]. These low-penetrance genetic risk variants may interact with either inherited or acquired mutations in *TP53* within the breast epithelium to promote or mitigate breast carcinogenesis. A total of forty-two single nucleotide polymorphisms have been associated with alterations in the penetrance of inherited mutations in *BRCA1/2* [5]. However, genetic polymorphisms that modify the penetrance of pathogenic *TP53* variants have been difficult to identify in humans. Rodent models bearing heterozygous deletions in *Trp53* also develop tumors in multiple tissues but exhibit striking differences in tumor spectrum among strains. In *Trp53*$^{+/−}$ rats, the incidence of mammary tumors ranged between 15-19% [6, 7]. Mammary carcinoma was rarely detected in C57BL/6-*Trp53*$^{+/−}$ mice [8-10]. In contrast, BALB/c-*Trp53*$^{+/−}$ mice developed spontaneous mammary tumors in 42-65% of females [11, 12]. This variation among inbred strains offers an opportunity to identify genetic modifiers that affect the incidence of breast tumors associated with Li-Fraumeni

syndrome. Polymorphisms that differ between BALB/c and C57BL/6 mice have been associated with differences in tumor susceptibility. A hypomorphic *Prkdc* allele was shown to promote radiation-sensitivity in BALB/c [13]. A polymorphism in *Cdkn2a/Ink4a* of BALB/c mice was also shown to have decreased activity of p16^{INK4a} and was associated with susceptibility to plasmacytomas induced by pristine [14]. However, neither the *Prkdc* nor *Cdkn2a* alleles in BALB/c were linked to differences in the incidence of mammary tumors in *Trp53*$^{+/-}$ mice [11].

High and medium penetrance inherited risk alleles for breast cancer predominantly affect double-strand break (DSB) repair and suggest a critical role of these pathways in determining susceptibility. DSBs result from oxidative damage, environmental irradiation as well as DNA replication. DSBs are repaired predominantly by non-homologous end joining (NHEJ) and homologous recombination (HR) pathways. In NHEJ, the DSB ends are protected rapidly by Ku70/80. This protein is recognized by DNA-PKcs (encoded by *Prkdc*) forming a synaptic complex of both ends of the DSB which is followed by end-ligation. NHEJ is potentially mutagenic because it relies on microhomologies that can lead to loss of nucleotides [15]. In contrast, repair at replicating forks predominantly takes place through HR [16]. In HR, DSBs undergo strand resection which generates 3'-ssDNA overhangs. A complex of BRCA1-PALB2-BRCA2 leads to the loading of RAD51 which facilitates strand exchange and DNA synthesis from a homologous donor strand [17]. Alternatively, DSBs with 3'-ssDNA tails can be repaired with error-prone repair pathways such as alternative end joining (aEJ) and single-strand annealing (SSA) which can lead to loss of nucleotide, and therefore, are non-conservative [18]. Increased reliance on SSA was associated with increased risk of breast cancer [19]. Therefore, the balance of the DSB repair pathways appear to play critical roles in maintaining genomic stability and conferring risk of breast cancer.

We previously identified two loci, *Suprmam1* on chromosome 7 and *Suprmam2* on chromosome 2 through genetic linkage analysis that contribute to development of mammary tumors in BALB/c-*Trp53*$^{+/-}$ mice [12, 20]. In the present study, the *Suprmam1* locus was fine mapped to a 10cM interval. The C57BL/6J alleles for this interval were introgressed into the BALB/cMed background to create the BALB/cMed.B6-*Suprmam1*(N10)-*Trp53*$^{tm1Tyj/+}$ congenic mice (designated SM1-*Trp53*$^{+/-}$). DNA damage and repair were compared in the SM1 and parental strains. BALB/cMed-*Trp53*$^{+/-}$ mice have a 2.5-fold greater reliance on single strand annealing (SSA) for repair of DNA double strand breaks compared to C57BL/6J-*Trp53*$^{+/-}$ mice. The C57BL/6J alleles in SM1-*Trp53*$^{+/-}$ mice were sufficient to revert levels of repair of DNA double strand breaks to that in the C57BL/6J-*Trp53*$^{+/-}$ parental strain. In contrast, radiation-induced damage in mammary epithelium of SM1-*Trp53*$^{+/-}$ mice did not differ from BALB/c-*Trp53*$^{+/-}$ mice suggesting that repair via non-homologous end-joining (NHEJ) is not linked to *Suprmam1*. Analysis of mRNA levels for DNA repair genes showed significant overlap between the C57BL/6J-*Trp53*$^{+/-}$ and SM1-*Trp53*$^{+/-}$ cells compared to those from BALB/cMed-*Trp53*$^{+/-}$. As these DNA repair genes are not linked to the *Suprmam1* locus, it suggests that the interval regulates a DNA repair program. BALB/cMed-*Trp53*$^{+/-}$ cells also exhibited slower replication rates compared to C57BL/6J-*Trp53*$^{+/-}$ which was complemented by *Suprmam1*$^{B6/B6}$ resulting in rates equivalent to the C57BL/6J-*Trp53*$^{+/-}$ cells. The results demonstrate that the *Suprmam1*

locus plays an important role in coordinating replication fork dynamics and selection of repair pathways which may contribute to the difference in susceptibility to mammary tumors in these mouse models of LFS.

Results

Fine mapping *Suprmam1* locus

Seventeen polymorphisms on mouse chromosome 7 were used to define the boundaries of the *Suprmam1* locus associated with spontaneous mammary tumors in [BALB/cMed.C57BL/6]N2-*Trp53*$^{+/-}$ backcross female mice. The linkage analysis suggests a complex locus (Fig. 1a). Strongest linkage was observed between presence of mammary tumors and a region bounded by rs32285976 (*Plekha7*) and rs32420445 (*Dock1*). The peak of this interval is at rs33080487 which lies within the *Rabep2* gene (133.58 MB, Table 1). The interval includes polymorphisms in *Jmjd5, Il4ra, Il21, Rabep2,* and *D7Mit105.* An adjacent peak is detected at rs3023153 raising the possibility that two separate modifiers exist within the *Suprmam1* locus. A multiple QTL model improved the overall LOD to 6.1 (Fig. 1b); however, significant epistasis was not detected among the QTLs.

The tumor spectrum for p53-deficient mice has been reported for C57BL/6, BALB/c, FVB, DBA/2 and 129Sv strains and only BALB/c exhibit a high frequency of spontaneous mammary tumors [10-12, 21-24]. The mouse phylogeny viewer (http://msub.csbio.unc.edu/) was used to compare haplotypes within the *Suprmam1* locus [25]. The majority of the *Suprmam1* interval between rs16789781 in *Nlrp14* and rs32420445 in *Dock1* (114-142 Mb) has substantial similarities among the strains. Although there was suggestive linkage with rs3023148 (Fig. 1a), the region adjacent to this polymorphism in *Rras2* (121 Mb) was largely conserved across the strains. In contrast, within the major peak of linkage bounded by *Plekha7* and *Dock1*, three regions were identified in which BALB/cJ alleles are unique compared to the strains that do not develop spontaneous mammary tumors when heterozygous for *Trp53* (Fig. 2a). Regions B (132-133.2 Mb) and C (134.5-136Mb) lie near the peak linkage on chromosome 7 surrounding *Rabep2* while Region A (125-127 Mb) lies at the centromeric boundary adjacent to *Abca14*. The region of mouse chromosome 7 surrounding *Rabep2* is syntenic to human chromosome 16 with the telomeric region of the interval being syntenic with chromosome 10 (Fig. 2b & c). These comparisons suggested that the region between *Plekha7* (123Mb) and *Dock1* (142Mb) is likely to harbor the polymorphisms underlying the differences in mammary tumors.

Marker-assisted selection was used to generate mice that were congenic for C57BL/6J alleles in the interval bounded by *Plekha7* and *Dock1*. The BALB/cMed.B6-*Suprmam1*(N10)-*Trp53*$^{tm1Tyj/+}$ congenic mice (designated SM1-*Trp53*$^{+/-}$ strain) are homozygous for C57BL/6J alleles in the *Suprmam1* interval in a genetic background that is otherwise BALB/cMed (Fig. 3a). To further define the interval, genotyping was performed using the Mouse Diversity Array (MDA) on DNA from BALB/cMed, C57BL/6J and SM1 mice. The SNPs were mapped to the mouse reference genome mm9. MDA integrates over 623,000 SNP to a resolution of 4.3kb. We observed the first breakpoint at Chr7:121816106-121851009 and second breakpoint at Chr7:141994734-142031773,

suggesting the minimal interval of C57BL/6J alleles introgressed in the SM1 strain stretches from 121851009 to 141994734 Mb (Fig. 3b).

Genes within the interval in SM1 mice involved in DNA damage and repair

The interval (chr7: 121851009 -141994734) codes for 212 annotated protein coding genes in the reference genome NCBIM37. We narrowed the number of candidate genes to 23 if the gene 1) had role in DNA damage, DNA repair, DNA replication or homologous recombination, 2) harbored a coding non-synonymous SNP or 3) orthologous to any genes associated with breast neoplasm (Table 2)[26]. The haplotype blocks B and C (132-133.2 and 134.5-136Mb) identified in Fig 2a were used to refine the evaluation of this list. Of the 3 genes within the SM1 interval associated with breast cancer in women (*Fgfr2*[27], *Ate1*[28], *Sty17*[29]), all lie outside the haplotype blocks unique to BALB/c. While *Palb2* is a candidate, it too lies outside the haplotype blocks and was unable to rescue the differences in DNA repair in previous work [30]. Within the B and C block *Nsmce1* and *Mcmbp* are DNA repair and replication genes, respectively. In addition, *Il21r* has a non-synonymous coding polymorphism and altering codon structure was found in *Itgal* and *Tgfb1i*. Expression of *Suprmam1* genes between C57BL/6-*Trp53*$^{+/-}$ and BALB/c-*Trp53*$^{+/-}$ mammary gland was previously analyzed by microarray by Blackburn et al., 2007 [20]. Only three genes (*Trm12*, *Thumpd1* and *DMbt1*) were found to be differentially expressed in that initial study. None of the genes from the list of 23 genes were differentially expressed between C57BL/6-*Trp53*$^{+/-}$ and BALB/c-*Trp53*$^{+/-}$. Therefore, the analysis of DNA sequences did not identify clear candidates with polymorphisms affecting functions related to DNA repair.

SM1 interval is not associated with radiation sensitivity

The BALB/c and C57BL/6 strains differ in their sensitivity to radiation-induced genomic instability which can modify susceptibility to tumors. BALB/c radiation sensitivity was mapped to 5 *Rapop* loci, none of which was in chromosome 7 [31-34]. Gene expression in mammary tissue from BALB/c and C57BL/6 mice treated with either low (7.5 cGy) or high doses(1.8 Gy) of irradiation for short (4h) or long treatment periods (weekly 4 weeks) [35] were compared to identify potential eQTLs among genes within the *Suprmam1* interval (Fig. 4a). Thirteen genes were differentially expressed between BALB/c and C57BL/6 in at least one of the conditions (Supplementary Table 1). Among these genes, strain-specific patterns of expression were observed with levels of *Thumpd1* being higher in BALB/c while *Prss8*, *Dmbt1, Gde1 and Tmem159* were lower compared to C57BL/6 (Fig. 4a). A long-range structural element may contribute to these differences, but the genes are dispersed over a large region from 125-138 Mb and vary in the levels of response to radiation. Radiation-induced expression of p53-dependent genes (*Cdkn1a*, *Bax* and *Mdm2*) was similar for both strains indicating that DNA damage response signaling is intact, but levels of induction were higher in BALB/c compared to C57BL/6.

Radiation-induced apoptosis was used as a functional test to evaluate differences in DNA damage in the mammary epithelium. This endpoint concomitantly assesses the proficiency of repair through the non-homologous end-joining pathway which repairs the majority of DSBs within 2h post-irradiation. Apoptosis occurs in cells with persistent DNA damage, and therefore, apoptosis was evaluated using the TUNEL assay 6h post-irradiation (Fig. 4b).

C57BL/6J-*Trp53*$^{+/−}$ mammary epithelium was highly resistant to irradiation (0.34% TUNEL-positive cells), whereas TUNEL-positive mammary epithelial cells were increased 20-fold in BALB/cMed-*Trp53*$^{+/−}$ (6.78 %) (p = 0.009, Fig. 4c, Supplementary Fig 1a). In SM1-*Trp53*$^{+/−}$ mice, 4.6% TUNEL-positive mammary epithelial cells were observed but the difference in apoptosis was not statistically significant (p = 0.8) compared to BALB/cMed-*Trp53*$^{+/−}$ mice. This appears to be a consequence of the greater acute and persistent DNA damage in mammary tissue of BALB/cMed-*Trp53*$^{+/−}$ mice but is not genetically linked to the *Suprmam* interval in SM1-*Trp53*$^{+/−}$ mice and does not modify the apoptotic responses.

The SM1 interval modifies homology-directed repair

BALB/cMed-*Trp53*$^{+/−}$ mice were previously shown to have a greater reliance on an error-prone pathway for repair of DSBs compared to C57BL/6J-*Trp53*$^{+/−}$ mice, by EGFP-reactivation assays using mammary epithelial cells (MEC) as well as MEFs [30]. In this assay, DSB repair was quantified by the reconstitution of functional EGFP (Fig. 5a) using a plasmid constructed to be repaired primarily by single-strand annealing (SSA). We observed 2.5-fold elevated SSA (% EGFP-positive among transfected live cells) in BALB/cMed-*Trp53*$^{+/−}$ compared to C57BL/6J-*Trp53*$^{+/−}$ MEFs. In contrast, SSA in SM1-*Trp53*$^{+−}$ was similar to that in C57BL/6J-*Trp53*$^{+/−}$ (Fig. 5b, Supplementary Fig 1b). Therefore, the alleles from the C57BL/6J background in the SM1 mice are sufficient to revert the levels of DSB repair via SSA to the low levels found in C57BL/6J-*Trp53*$^{+/−}$ mice.

A panel of 24 genes that contribute to differences in repair by SSA were identified in an siRNA screen in C57BL/6 and BALB/cMed using the EGFP-reactivation assay [30]. To determine if expression of these genes may be associated with the *Suprmam1* interval, we determine mRNA levels of the 24 genes in mouse MEFs from BALB/cMed-*Trp53*$^{+/−}$, C57BL/6J-*Trp53*$^{+/−}$ and SM1-*Trp53*$^{+/−}$ mice. We found that 6 genes (*Rev1*, *Rev3l*, *Ercc5*, *Rdm1*, *Pole3* and *Trex2*) were differentially expressed between the parental strains and that their expression in SM1-*Trp53*$^{+/−}$ mice was similar to that in the C57BL/6J-*Trp53*$^{+/−}$ cells (Fig. 5c). Hierarchical clustering was used to evaluate the relationships of expression among the 24 genes in these strains and showed that expression was most similar in SM1-*Trp53*$^{+/−}$ and C57BL/6J -*Trp53*$^{+/−}$. Correlation analysis (Fig. 5d) shows that the overall pattern of the DNA repair genes in SM1-*Trp53*$^{+/−}$ was more similar to that of C57BL/6-*Trp53*$^{+/−}$ with spearman's rank correlation coefficient (rs) 0.77 (p < 7.376294 X $10^{−6}$) than BALB/c-*Trp53*$^{+/−}$(rs = 0.27 p =0.19). As these genes lie on other chromosomes and are not physically linked to the *Suprmam1* interval, the results suggest that the *Suprmam1*$^{B6/B6}$ alleles coordinate a DNA repair program that limits the levels of repair of DSBs through the error-prone SSA mechanism.

The SM1 interval regulates replication-fork processivity

The SM1 interval contains genes involved in DNA replication (Table 2) and DNA polymerases involved in translesion synthesis and the Fanconi Anemia (FA) pathway were enriched among the panel of 24 genes that differentially regulate DSB repair in BALB/cMed-*Trp53*$^{+/−}$ and C57BL/6J-*Trp53*$^{+/−}$ cells [30]. Fanconi Anemia (FA) pathway, which is involved in intra-strand crosslink repair, was found to be defective in BALB/cMed-*Trp53*$^{+/−}$. Therefore, DNA fiber assays were used to evaluate replication fork activities and the effect

of DNA intra-strand crosslinking by Mitomycin C (MMC) (Fig. 6a, b & Supplementary Fig 1c). The median length of replication tracts in BALB/cMed-$Trp53^{+/-}$ MEFs was significantly shorter than that of C57BL/6J-$Trp53^{+/-}$ MEFs (6.07 and 8.25 μm respectively, difference = 2.18 μm, p = 7.5 x 10^{-22}). In contrast, the replication tract length in SM1-$Trp53^{+/-}$ MEFs (8.29 μM) did not differ from that in C57BL/6J-$Trp53^{+/-}$ MEFs (difference = 0.4 μm, $p = 0.9$) but was significantly longer than BALB/cMed-$Trp53^{+/-}$ MEFs (difference 2.22 μm, p = 2.2 x 10^{-17}). Therefore, C57BL/6J alleles in the SM1 interval were sufficient to rescue replication fork kinetics (Fig 6c).

Crosslinking of DNA using MMC reduced replication tract lengths in all strains compared to the untreated cultures. The median tract length with MMC treatments for BALB/cMed-$Trp53^{+/-}$, C57BL/6J-$Trp53^{+/}$ and SM1-$Trp53^{+/}$ were 6.62, 4.38 and 5.68 μM respectively (Fig 6d). Although it was anticipated that the BALB/cMed-$Trp53^{+/-}$ MEFs may be more sensitive to MMC, all strains were affected similarly (difference in median fork length = 1.3 μm) suggesting that both C67BL/6J and BALB/cMed are equally susceptible to DNA crosslinking. However, the relative effects of genetic backgrounds on DNA replication processivity remained evident with median replication fork lengths shorter in BALB/cMed-$Trp53^{+/-}$ compared to C57BL/6J-$Trp53^{+/-}$ or SM1-$Trp53^{+/-}$ (2.24 μm, p = 6.60 x 10^{-11}; 1.3 μm, p = 2.46 x 10^{-9}), but no difference in median replication fork length between C57BL/6J and SM1 (0.06 μm; p = 0.8). Therefore, the SM1 interval regulates processivity of DNA replication but does not alter bypass DNA crosslinks specifically.

Discussion

Mutation of the *TP53* gene is the most common genetic alteration found in human cancers. Somatic mutations in *TP53* were consistently observed in the pan-cancer cohort of 3,281 tumors across 12 tissues including breast cancers [36]. Analysis of TCGA data shows significant co-occurence of mutations in genes regulating the cell cycle (e.g. *MYC, TERT, PTEN, CSMD1*) with *TP53* mutations in breast cancers [37]. Similar results have been obtained in multiple cancers from TGCA datasets, as well as in p53-null mouse models in which most thymic lymphoma exhibit mutation in these genes [38]. This suggests that there are pathways that can compensate for loss of p53 function and complementary mutations are required to allow initiation and progression of tumors.

Heterozygous mutation of *Trp53* in BALB/cMed mice confers a striking sensitivity to mammary tumors compared to C57BL/6 mice providing an opportunity to identify the genetic basis for variable penetrance. These pathways can provide insights into those that modify the impact of *TP53* mutations in human breast cancers. Linkage analysis defined a minimal interval on chromosome 7 centered around polymorphisms in the *Rabep2* gene, a secondary peak associated with a polymorphism in the *Rras2* gene (Fig. 1a) and a *Suprmam2* on chromosome 2 that contribute to the susceptibility to mammary tumors in BALB/cMed and resistance in C57BL/6J mice [20]. These loci appear to act in an additive manner to determine risk of mammary tumors. Breast cancer is a complex trait in humans with >180 risk alleles detected in GWAS and susceptibility to mammary tumors in mice appears to be a similarly complex trait with multiple polymorphisms modifying the

consequences of haploinsufficiency for *Trp53* in the mammary epithelium but not in other tissues.

As heritable susceptibility to breast cancer is associated with mutations in genes involved in DSB repair and has been linked with a shift to error-prone homology-directed repair [30] , we determined the effect of the *Suprmam1* alleles on removal of radiation-induced damage and homology-directed repair. Differences in sensitivity to ionizing radiation between C57BL/6 and BALB/c have been reported previously [39]. Although radiation-induced apoptosis was significantly greater in the mammary epithelium of BALB/cMed-*Trp53*$^{+/-}$ mice than in C57BL/6J-*Trp53*$^{+/-}$, the *Suprmam1*$^{B6/B6}$ allele did not rescue apoptosis in SM1-*Trp53*$^{+/-}$ mice (Fig. 4b). The greater radiation-induced apoptosis appears to be due to the hypomorphic expression of the BALB/c allele of *Prkdc* affecting repair of DSBs by the NHEJ pathway [40] and is not linked to mammary tumor susceptibility [11].

DSBs are also repaired by homology-directed repair pathways. Canonical homologous recombination is a conservative repair mechanism that requires BRCA1, BRCA2, PALB2 and mutations in these are associated with familial breast cancer. Alternate pathways can compensate for deficiencies in these genes but mediate error-prone repair. BALB/cMed-*Trp53*$^{+/-}$ mice were shown to preferentially use the homology-directed SSA pathway [30]. The C57BL/6J alleles in SM1-*Trp53*$^{+/-}$ congenic mice were sufficient to rescue the low levels of SSA observed in the parental C57BL/6J-*Trp53*$^{+/-}$ mice (Fig 5b) indicating the role of this interval in suppressing error-prone repair of DSBs. Homology-directed repair is active in cells undergoing DNA replication suggesting that replication stress may contribute to the repair phenotype. DNA fiber assays were used to assess replication fork dynamics. In BALB/cMed-*Trp53*$^{+/-}$cells, rates of replication fork progression were decreased compared to the C57BL/6J-*Trp53*$^{+/-}$ (Fig. 6c). This phenotype was also rescued in the SM1-*Trp53*$^{+/-}$ cells. Genetic complementation of both the DSB repair via SSA and replication fork dynamics by the C57BL/6J alleles in the SM1 strain suggests that these 2 phenotypes may be the result of a single genetic difference linked to the SM1 interval.

The genes within the *Suprmam1* locus provide candidates for regulating the differences in replication and repair between these strains of mice. *Palb2* lies within the interval and was shown to interact with deletion of *Trp53* to accelerate mammary tumors in mice [41]. However, *Palb2* is distant from the region with strongest linkage (Fig. 1) and is positioned within haplotype blocks that are shared among BALB/c as well as strains that do not develop mammary tumors when heterozygous for *Trp53* (Fig. 2). Functional complementation by overexpression of the cDNA from C57BL/6J also failed to alter the repair via SSA in BALB/cMed-*Trp53*$^{+/-}$ MEFs [30]. The *DMBT1* gene has also been implicated in breast cancer risk [20, 42], but it also lies distant from markers with the highest LOD scores. In humans, loss of heterozygosity in *DMBT1* is associated with loss of the adjacent *PTEN* gene on chromosome 16 [43]. However, the mouse *Pten* gene is located on mouse chromosome 19, and therefore, unlinked to the *Suprmam1* interval. Mammary tumors were analyzed for markers within the *Suprmam1* interval, but there was no apparent loss of heterozygosity detected. While the interval contains genes involved in DNA replication and repair, none had polymorphisms that disrupt their function (Table 2). The interval harbors 4 genes that are differentially responsive to ionizing radiation and lie within haplotype blocks that differ in

BALB/c vs other strains (Fig. 4a) but appear to be secondary to differerences in NHEJ that are not linked to the SM1 interval based on the failure to rescue the low levels of apoptosis observed in the parental C57BL/6J-*Trp53*$^{+/-}$ mice (Fig. 4c). In contrast, a panel of genes involved in DNA repair and shown to contribute to the differences in DSB repair mediated by SSA in BALB/cMed*Trp53*$^{+/-}$ compared to C57BL/6J-*Trp53*$^{+/-}$ was modified by the SM1 interval (Fig 5c, 5d). The SM1-*Trp53*$^{+/-}$ expression pattern was strongly correlated with that in C57BL/6-*Trp53*$^{+/-}$ and differed from that in BALB/cMed-*Trp53*$^{+/-}$. Thus, the *Suprmam1*$^{B6/B6}$ alleles appear to drive expression of a DNA repair program that includes *Rev1, Rev3l, Rdm1, Ercc5, Pole3* and *Trex2* genes, i.e. including two translesion synthesis and one replicative polymerase subunit.

The overall observations identify replication stress and reliance on error-prone DNA repair by SSA is linked to the *Suprmam1* interval in the tumor-susceptible BALB/c strain. Reliance on SSA has also been associated with increased risk of breast and ovarian cancer in women [19, 44]. But the tissue specificity of disruptions in homology-directed repair remain a significant question as increased error-prone DNA repair in BALB/cMed-*Trp53*$^{+/-}$ mice would increase the potential for pathogenic mutations in all tissues. The estrogen receptor α (ERα) has been shown to induce DSBs in breast cancer cell lines and in the mammary epithelium of BALB/c mice even in the absence of proliferation [45]. Therefore, the luminal cells of the mammary epithelium would be subjected to continuous DNA damage which, together with the replication stress and error-prone repair through SSA, would increase the probability of acquiring oncogenic mutations [46].

The *Suprmam1* interval identifies a novel DNA repair program and pathway that can potentially contribute to breast cancer susceptibility in humans. The DNA repair program may be coordinated by a transcription factor or a microRNA gene within this interval. Alternatively, the *Suprmam1* interval may harbor a structural element that modifies chromatin organization [47] and regulates expression of a transcription factor or microRNA that lies outside the *Suprmam1* interval. The DSB repair and DNA fiber assays can be used in MEFs bearing recombinations within the interval to isolate the minimal region controlling these phenotypes. These functional assays can also be applied to cells from LFS patients to assess the effect of these mechanisms on penetrance and cancer spectrum.

Materials and Methods

Animals

All animal procedures were in accordance with the national guidelines for the care and use of animals and approved by the University of Massachusetts Amherst's Institutional Animal Care and Use Committee. The BALB/c mice used throughout were obtained from Daniel Medina (Baylor College of Medicine, Houston, TX) and have been maintained as a closed colony, and thus, are referred to as BALB/cMed. The *Trp53*^{tm1Ty} null allele was backcrossed onto the BALB/c genetic background for 11 generations [21]. The *Trp53*^{tm1Ty} knockout allele was used in these studies and heterozygous mice are referred to subsequently as *Trp53*$^{+/-}$.

Linkage mapping

The panel of N2 backcross mice used for linkage mapping was described previously [20]. Briefly, [C57BL/6J x BALB/cMed]-F1-*Trp53*^{+/+} females were backcrossed with BALB/cMed-*Trp53*^{−/−} males to generate a panel of 188 female [(C57BL/6Jx BALB/cMed) x BALB/cMed]-N2-*Trp53*^{+/−} mice. These mice were monitored for development of mammary tumors and were scored using a binary phenotype for the presence or absence of tumors, as well as a quantitative measurement of the number of days until tumor detection. DNA samples from these mice were genotyped for polymorphisms in 17 markers. Sample size, inclusion/exclusion criteria for mammary tumor phenotype and genotyping method for ten markers on chromosome 7 were described previously [20]. Genotypying methods for 7 additional SNPs are described in Supplementary Table 2. Four markers within *Suprmam2* on chr2 and coding polymorphisms that differ between the 2 parental strains in *Cdkna2a* (chr4) and *Prkdc* (chr16) [11, 20] were included to assess possible epistatic interactions. Gentoyping conditions are described Supplementary material and methods.

The data were analyzed using R/qtl [48] for both binary and quantitative tumor phenotypes; however, the quantitative assessment of days to tumor formation yielded no significant linkages. The positions of markers were defined using recombination maps for females based on NCBI Build 37/mm9 (http://cgd.jax.org/mousemapconverter/); marker DNA sequence was used to identify alternate markers with the identical polymorphism in cases where the scored marker was not present in the mousemapconverter set. Linkage was determined using simple regression, interval mapping, and a multiple QTL models that included the locus on chromosome 2 [20, 49]. These linkage methods adjust the positions of markers for the recombination observed within the backcross population.

Generation of the SM1 congenic mouse strain

Wild type BALB/cMed and C57BL/6J mice were intercrossed to generate F1 progeny. These mice were backcrossed to BALB/cMed to generate 239 N2 progeny. The N2 mice were screened for polymorphisms in *Plekha7, Tmc5, Abca14, Jmjd5, IL21r, Rabep2, Dock1* genes to identify mice heterozygous for C57BL/6J and BALB/cMed alleles within the *Suprmam1* locus on chromosome 7. N2 founders 179 and 216 were heterozygous for markers between *Plekha7* and *Dock1*. These lines were backcrossed with BALB/cMed to produce N3 and N4 mice heterozygous for all markers. N4 female mice were crossed with BALB/cMed-*Trp53*^{−/−} males to generate N5-*Trp53*^{+/−} mice. Backcrossing with wild type BALB/cMed-*Trp53*^{−/−} mice continued with selection for heterozygosity of all 7 markers through N10 for both line 179 and 216. Mice within each line (179 and 216) were crossed to create the BALB/cMed.B6-*Suprmam1*(N10)-*Trp53*[tm1Tyj/+] strain, referred to as SM1-*Trp53*^{+/−}, that is homozygous for C57BL/6J alleles across the interval bounded by *Plekha7* and *Dock1*. Mice from Line 216 were used in the experiments presented. Line 179 was cryopreserved but not used for further analyses.

Genotyping using the mouse diversity array

Genomic DNA was isolated from liver or intestinal tissues from each strain. Genotyping was performed by Genome Explorations (Memphis, TN) using Mouse Diversity Array (cat #520650, Affymetrix, Santa Clara, CA) and the SNP 6.0 Assay reagent kit (cat #460004,

Affymetrix) according to the manufacturer's instructions. Genotypes were determined using the MouseDivGeno R package [50].

Cell culture

Mouse embryonic fibroblasts (MEFs) were collected from C57BL/6-*Trp53*^{+/−}, BALB/cMed-*Trp53*^{+/−} and SM1-*Trp53*^{+/−} mice as described previously [51]. Detailed procedure for the MEF collection and culture is described in Supplementary material and methods.

Terminal deoxynucleotidyl transferase dUTP nick end labeling (*TUNEL*) assay

Mice of age 8 weeks were ovariectomized and allowed to recover for one week for the endogenous hormones to reach baseline level. The mice were then treated with estrogen plus progesterone to enhance p53-mediated apoptotic responses [52]. Medical grade silastic tubing was cut to a length of 1.2 cm and filled with 50 μg 17-β-estradiol (cat #E2758-1G, Sigma-Aldrich, St. Louis, MO) and 20 mg of progesterone (cat #P0130-25G, Sigma-Aldrich). Both ends were sealed with clear silicone. Capsules were implanted subcutaneously on the dorsal side of the mouse, 1/2 inch distal to the neck. On the fourth day after implantation, mice were subjected to 5 Gy ionizing irradiation from a ^{137}Cs source. Six hours later, the mice were sacrificed, the fourth mammary glands were harvested, fixed in 10% neutral-buffered formalin (NBF) and embedded in paraffin. Sections of paraffin embedded mammary glands were subjected to TUNEL assay using ApopTag Plus Peroxidase In Situ Apoptosis Kit (cat #S7101, Sigma-Aldrich). A total of 1200 epithelial cells were counted per slide with >6 mice analyzed for each treatment x genotype combination.

EGFP-reactivation Assay

DNA repair by EGFP-reactivation assays were performed as described previously [53]. The EGFP/3'EGFP construct used in these studies measures repair primarily through single-strand annealing (SSA) mechanism and only a small proportion through conservative homologous recombination. The assay procedure is described in detail in Supplementary Material and Methods.

DNA fiber assay

MEFs were pulse labeled with 25 μM 5-chloro-2'-deoxyuridine (cat #C6891, Sigma-Aldrich,) and 250 μM 5-iodo 2'-deoxyuridine (cat #I7125-5G, Sigma-Aldrich) successively for the indicated times, with or without additional replication stress using 8 μM Mitomycin-C (MMC, cat #M0503, Sigma Aldrich). DNA fiber spreading, immunostraning and quantification is described in Supplementary Material and Methods.

Evaluation of candidate genes

Evaluation of genes within SM1 interval for their possible role in mammary tumor is done using either 1) role in DNA repair, 2) presence of non-synonymous coding variants or 3) orthologous to GWAS variants associated with breast neoplasm. The detailed procedure is described in Supplementary Materials and Methods.

Statistical analysis

Student's t-test were performed to analyze the gene expression of DNA repair genes. Correlation testing of the 24 DNA repair gene expression between strains were performed with spearman's rank-ordered correlation analysis. Results from TUNEL, EGFP reactivation assays and DNA fiber assays were analyzed with Kruskal-Wallis analysis of variance (ANOVA). Once statistical significance was established for a data set by Kruskal-Wallis test, non-parametric Mann-Whitney test for unpaired samples was applied on the result of EGFP reactivation assay using GraphPad Prism (GraphPad, San Diego, CA, USA). For post-hoc comparisons of TUNEL positive cells and replication tract length between strains, dunn's test were applied in R using FSA package. * $p < 0.05$; ** $p < 0.01$; *** $p < 0.001$; **** $p < 0.0001$.

Code availability

All computer code is available upon request

Supplementary Material

Refer to Web version on PubMed Central for supplementary material.

Acknowledgements:

References

1. Bouaoun L, Sonkin D, Ardin M, Hollstein M, Byrnes G, Zavadil J et al. TP53 Variations in Human Cancers: New Lessons from the IARC TP53 Database and Genomics Data. Hum Mutat 2016; 37: 865–876. [PubMed: 27328919]

2. Amadou A, Achatz MIW, Hainaut P. Revisiting tumor patterns and penetrance in germline TP53 mutation carriers: temporal phases of Li-Fraumeni syndrome. Curr Opin Oncol 2018; 30: 23–29. [PubMed: 29076966]

3. Fortuno C, James PA, Spurdle AB. Current review of TP53 pathogenic germline variants in breast cancer patients outside Li-Fraumeni syndrome. Human mutation 2018; 39: 1764–1773. [PubMed: 30240537]

4. Wendt C, Margolin S. Identifying breast cancer susceptibility genes - a review of the genetic background in familial breast cancer. Acta oncologica (Stockholm, Sweden) 2019; 58: 135–146.

5. Milne RL, Antoniou AC. Modifiers of breast and ovarian cancer risks for BRCA1 and BRCA2 mutation carriers. Endocr Relat Cancer 2016; 23: T69–84. [PubMed: 27528622]

6. Yan HX, Wu HP, Ashton C, Tong C, Ying QL. Rats deficient for p53 are susceptible to spontaneous and carcinogen-induced tumorigenesis. Carcinogenesis 2012; 33: 2001–2005. [PubMed: 22791818]

7. Hansen SA, Hart ML, Busi S, Parker T, Goerndt A, Jones K et al. Fischer-344 Tp53-knockout rats exhibit a high rate of bone and brain neoplasia with frequent metastasis. Dis Model Mech 2016; 9: 1139–1146. [PubMed: 27528400]

8. Jacks T, Remington L, Williams BO, Schmitt EM, Halachmi S, Bronson RT et al. Tumor spectrum analysis in p53-mutant mice. Curr Biol 1994; 4: 1–7. [PubMed: 7922305]

9. Lang GA, Iwakuma T, Suh YA, Liu G, Rao VA, Parant JM et al. Gain of function of a p53 hot spot mutation in a mouse model of Li-Fraumeni syndrome. Cell 2004; 119: 861–872. [PubMed: 15607981]

10. Donehower LA, Harvey M, Vogel H, McArthur MJ, Montgomery CA, Park SH et al. Effects of genetic background on tumorigenesis in p53-deficient mice. Molecular carcinogenesis 1995; 14: 16–22. [PubMed: 7546219]

11. Blackburn AC, Brown JS, Naber SP, Otis CN, Wood JT, Jerry JD. BALB/c alleles for Prkdc and Cdkn2a interact to modify tumor susceptibility in Trp53+/− mice. Cancer research 2003; 63: 2364–2368. [PubMed: 12750252]

12. Koch JG, Gu X, Han Y, El-Naggar AK, Olson MV, Medina D et al. Mammary tumor modifiers in BALB/cJ mice heterozygous for p53. Mammalian Genome 2007; 18: 300–309. [PubMed: 17557176]

13. Yu Y, Okayasu R, Weil MM, Silver A, McCarthy M, Zabriskie R et al. Elevated breast cancer risk in irradiated BALB/c mice associates with unique functional polymorphism of the Prkdc (DNA-dependent protein kinase catalytic subunit) gene. Cancer research 2001; 61: 1820–1824. [PubMed: 11280730]

14. Zhang SL, DuBois W, Ramsay ES, Bliskovski V, Morse HC 3rd, Taddesse-Heath L et al. Efficiency alleles of the Pctr1 modifier locus for plasmacytoma susceptibility. Mol Cell Biol 2001; 21: 310–318. [PubMed: 11113205]

15. Chang HHY, Pannunzio NR, Adachi N, Lieber MR. Non-homologous DNA end joining and alternative pathways to double-strand break repair. Nat Rev Mol Cell Biol 2017; 18: 495–506. [PubMed: 28512351]

16. Karanam K, Kafri R, Loewer A, Lahav G. Quantitative live cell imaging reveals a gradual shift between DNA repair mechanisms and a maximal use of HR in mid S phase. Molecular cell 2012; 47: 320–329. [PubMed: 22841003]

17. Chen JJ, Silver D, Cantor S, Livingston DM, Scully R. BRCA1, BRCA2, and Rad51 operate in a common DNA damage response pathway. Cancer Res 1999; 59: 1752s–1756s. [PubMed: 10197592]

18. Scully R, Panday A, Elango R, Willis NA. DNA double-strand break repair-pathway choice in somatic mammalian cells. Nat Rev Mol Cell Biol 2019; 20: 698–714. [PubMed: 31263220]

19. Keimling M, Deniz M, Varga D, Stahl A, Schrezenmeier H, Kreienberg R et al. The power of DNA double-strand break (DSB) repair testing to predict breast cancer susceptibility. FASEB J 2012; 26: 2094–2104. [PubMed: 22278937]

20. Blackburn AC, Hill LZ, Roberts AL, Wang J, Aud D, Jung J et al. Genetic Mapping in Mice Identifies DMBT1 as a Candidate Modifier of Mammary Tumors and Breast Cancer Risk. The American Journal of Pathology 2007; 170: 2030–2041. [PubMed: 17525270]

21. Kuperwasser C, Hurlbut GD, Kittrell FS, Dickinson ES, Laucirica R, Medina D et al. Development of spontaneous mammary tumors in BALB/c p53 heterozygous mice. A model for Li-Fraumeni syndrome. The American journal of pathology 2000; 157: 2151–2159. [PubMed: 11106587]

22. Backlund MG, Trasti SL, Backlund DC, Cressman VL, Godfrey V, Koller BH. Impact of ionizing radiation and genetic background on mammary tumorigenesis in p53-deficient mice. Cancer Res 2001; 61: 6577–6582. [PubMed: 11522657]

23. Li B, Rosen JM, McMenamin-Balano J, Muller WJ, Perkins AS. neu/ERBB2 cooperates with p53-172H during mammary tumorigenesis in transgenic mice. Molecular and cellular biology 1997; 17: 3155–3163. [PubMed: 9154814]

24. Li Y, Halliwill KD, Adams CJ, Iyer V, Riva L, Mamunur R et al. Mutational signatures in tumours induced by high and low energy radiation in Trp53 deficient mice. Nature Communications 2020; 11: 394.

25. Wang JR, de Villena FP, McMillan L. Comparative analysis and visualization of multiple collinear genomes. BMC Bioinformatics 2012; 13 Suppl 3: S13.

26. Ramos EM, Hoffman D, Junkins HA, Maglott D, Phan L, Sherry ST et al. Phenotype-Genotype Integrator (PheGenI): synthesizing genome-wide association study (GWAS) data with existing genomic resources. Eur J Hum Genet 2014; 22: 144–147. [PubMed: 23695286]

27. Michailidou K, Hall P, Gonzalez-Neira A, Ghoussaini M, Dennis J, Milne RL et al. Large-scale genotyping identifies 41 new loci associated with breast cancer risk. Nature genetics 2013; 45: 353-361, 361e351-352. [PubMed: 23535729]

28. Fletcher O, Johnson N, Orr N, Hosking FJ, Gibson LJ, Walker K et al. Novel breast cancer susceptibility locus at 9q31.2: results of a genome-wide association study. J Natl Cancer Inst 2011; 103: 425–435. [PubMed: 21263130]

29. Hunter DJ, Kraft P, Jacobs KB, Cox DG, Yeager M, Hankinson SE et al. A genome-wide association study identifies alleles in FGFR2 associated with risk of sporadic postmenopausal breast cancer. Nature genetics 2007; 39: 870–874. [PubMed: 17529973]

30. Bohringer M, Obermeier K, Griner N, Waldraff D, Dickinson E, Eirich K et al. siRNA screening identifies differences in the Fanconi anemia pathway in BALB/c-Trp53+/− with susceptibility versus C57BL/6-Trp53+/− mice with resistance to mammary tumors. Oncogene 2013; 32: 5458–5470. [PubMed: 23435420]

31. Weil MM, Xia X, Lin Y, Stephens LC, Amos CI. Identification of quantitative trait loci controlling levels of radiation-induced thymocyte apoptosis in mice. Genomics 1997; 45: 626–628. [PubMed: 9367689]

32. Weil MM, Xia C, Xia X, Gu X, Amos CI, Mason KA. A chromosome 15 quantitative trait locus controls levels of radiation-induced jejunal crypt cell apoptosis in mice. Genomics 2001; 72: 73–77. [PubMed: 11247668]

33. Mori N, Okumoto M, van Der Valk MA, Imai S, Haga S, Esaki K et al. Genetic dissection of susceptibility to radiation-induced apoptosis of thymocytes and mapping of Rapop1, a novel susceptibility gene. Genomics 1995; 25: 609–614. [PubMed: 7759093]

34. Mori N, Okumoto M, Hart AA, Demant P. Apoptosis susceptibility genes on mouse chromosome 9 (Rapop2) and chromosome 3 (Rapop3). Genomics 1995; 30: 553–557. [PubMed: 8825642]

35. Snijders AM, Marchetti F, Bhatnagar S, Duru N, Han J, Hu Z et al. Genetic differences in transcript responses to low-dose ionizing radiation identify tissue functions associated with breast cancer susceptibility. PLoS One 2012; 7: e45394. [PubMed: 23077491]

36. Kandoth C, McLellan MD, Vandin F, Ye K, Niu B, Lu C et al. Mutational landscape and significance across 12 major cancer types. Nature 2013; 502: 333–339. [PubMed: 24132290]

37. Donehower LA, Soussi T, Korkut A, Liu Y, Schultz A, Cardenas M et al. Integrated Analysis of TP53 Gene and Pathway Alterations in The Cancer Genome Atlas. Cell Rep 2019; 28: 3010. [PubMed: 31509758]

38. Dudgeon C, Chan C, Kang W, Sun Y, Emerson R, Robins H et al. The evolution of thymic lymphomas in p53 knockout mice. Genes Dev 2014; 28: 2613–2620. [PubMed: 25452272]

39. Ullrich RL, Bowles ND, Satterfield LC, Davis CM. Strain-dependent susceptibility to radiation-induced mammary cancer is a result of differences in epithelial cell sensitivity to transformation. Radiat Res 1996; 146: 353–355. [PubMed: 8752316]

40. Okayasu R, Suetomi K, Yu Y, Silver A, Bedford JS, Cox R et al. A deficiency in DNA repair and DNA-PKcs expression in the radiosensitive BALB/c mouse. Cancer research 2000; 60: 4342–4345. [PubMed: 10969773]

41. Bowman-Colin C, Xia B, Bunting S, Klijn C, Drost R, Bouwman P et al. Palb2 synergizes with Trp53 to suppress mammary tumor formation in a model of inherited breast cancer. ProcNatlAcadSciUSA 2013.

42. Tchatchou S, Riedel A, Lyer S, Schmutzhard J, Strobel-Freidekind O, Gronert-Sum S et al. Identification of a DMBT1 polymorphism associated with increased breast cancer risk and decreased promoter activity. Human Mutation 2010; 31: 60–66. [PubMed: 19830809]

43. Sasaki H, Zlatescu MC, Betensky RA, Ino Y, Cairncross JG, Louis DN. PTEN is a target of chromosome 10q loss in anaplastic oligodendrogliomas and PTEN alterations are associated with poor prognosis. Am J Pathol 2001; 159: 359–367. [PubMed: 11438483]

44. Deniz M, Romashova T, Kostezka S, Faul A, Gundelach T, Moreno-Villanueva M et al. Increased single-strand annealing rather than non-homologous end-joining predicts hereditary ovarian carcinoma. Oncotarget 2017; 8: 98660–98676. [PubMed: 29228718]

45. Majhi PD, Sharma A, Roberts AL, Daniele E, Majewski AR, Chuong LM et al. Effects of Benzophenone-3 and Propylparaben on Estrogen Receptor-Dependent R-Loops and DNA Damage

in Breast Epithelial Cells and Mice. Environ Health Perspect 2020; 128: 17002. [PubMed: 31939680]

46. Jalan M, Olsen KS, Powell SN. Emerging Roles of RAD52 in Genome Maintenance. Cancers 2019; 11: 1038.

47. Schoenfelder S, Fraser P. Long-range enhancer-promoter contacts in gene expression control. Nat Rev Genet 2019; 20: 437–455. [PubMed: 31086298]

48. Broman KW, Wu H, Sen S, Churchill GA. R/qtl: QTL mapping in experimental crosses. Bioinformatics 2003; 19: 889–890. [PubMed: 12724300]

49. Ratnadiwakara M, Rooke M, Ohms SJ, French HJ, Williams RBH, Li RW et al. The SuprMam1 breast cancer susceptibility locus disrupts the vitamin D/ calcium/ parathyroid hormone pathway and alters bone structure in congenic mice. The Journal of Steroid Biochemistry and Molecular Biology 2018; 188: 48–58. [PubMed: 30529760]

50. Didion JP, Yang H, Sheppard K, Fu CP, McMillan L, de Villena FP et al. Discovery of novel variants in genotyping arrays improves genotype retention and reduces ascertainment bias. BMC Genomics 2012; 13: 34. [PubMed: 22260749]

51. Xu J. Preparation, culture, and immortalization of mouse embryonic fibroblasts. Curr Protoc Mol Biol 2005; Chapter 28: Unit 28 21.

52. Becker KA, Lu S, Dickinson ES, Dunphy KA, Mathews L, Schneider SS et al. Estrogen and progesterone regulate radiation-induced p53 activity in mammary epithelium through TGF-β-dependent pathways. Oncogene 2005; 24: 6345–6353. [PubMed: 15940247]

53. Akyuz N, Boehden GS, Susse S, Rimek A, Preuss U, Scheidtmann KH et al. DNA substrate dependence of p53-mediated regulation of double-strand break repair. Mol Cell Biol 2002; 22: 6306–6317. [PubMed: 12167722]

54. Kolishovski G, Lamoureux A, Hale P, Richardson JE, Recla JM, Adesanya O et al. The JAX Synteny Browser for mouse-human comparative genomics. Mamm Genome 2019; 30: 353–361. [PubMed: 31776723]
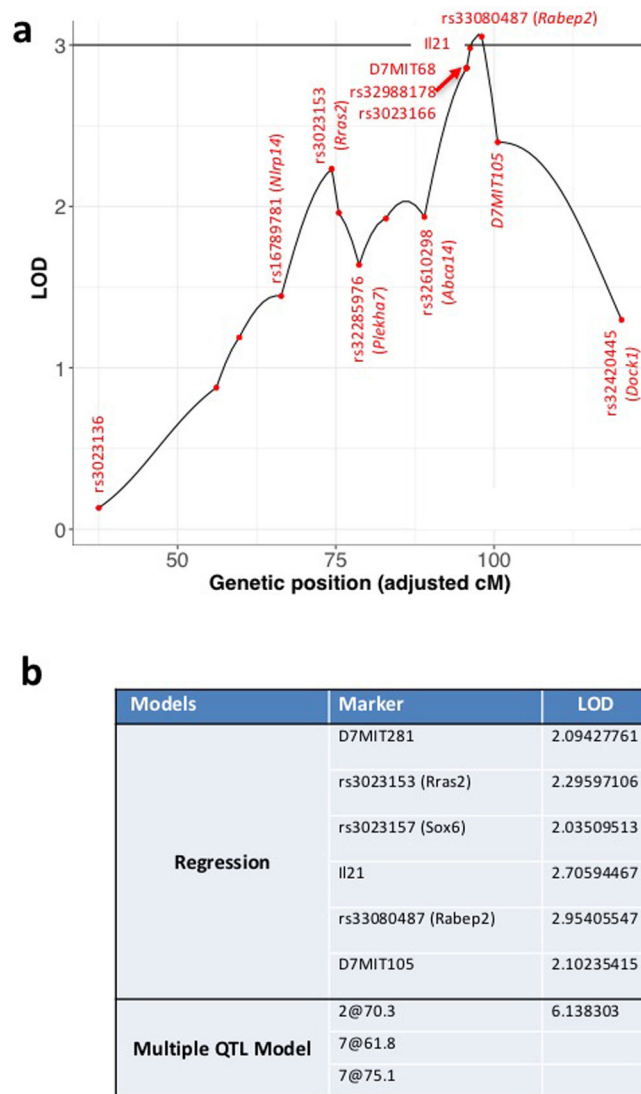
Models	Marker	LOD
Regression	D7MIT281	2.09427761
	rs3023153 (Rras2)	2.29597106
	rs3023157 (Sox6)	2.03509513
	Il21	2.70594467
	rs33080487 (Rabep2)	2.95405547
	D7MIT105	2.10235415
Multiple QTL Model	2@70.3	6.138303
	7@61.8	
	7@75.1	

Figure 1: Linkage analysis of mammary tumor incidence in BALB/cMed mice.
a) Linkage analysis of markers in the *Suprmam1* interval associated with mammary tumors. The line indicates linkage using interval mapping relative to positions of markers in cM based on recombination maps in female mice. b) Markers used in the linkage analysis using regression model and imputed marker position of multiple qtl model along with LOD scores. The multiple QTL model was used to assess the combined linkage estimates for the *Suprmam1* locus on chromosome 7 and *Suprmam2* locus on chromosome 2 together.
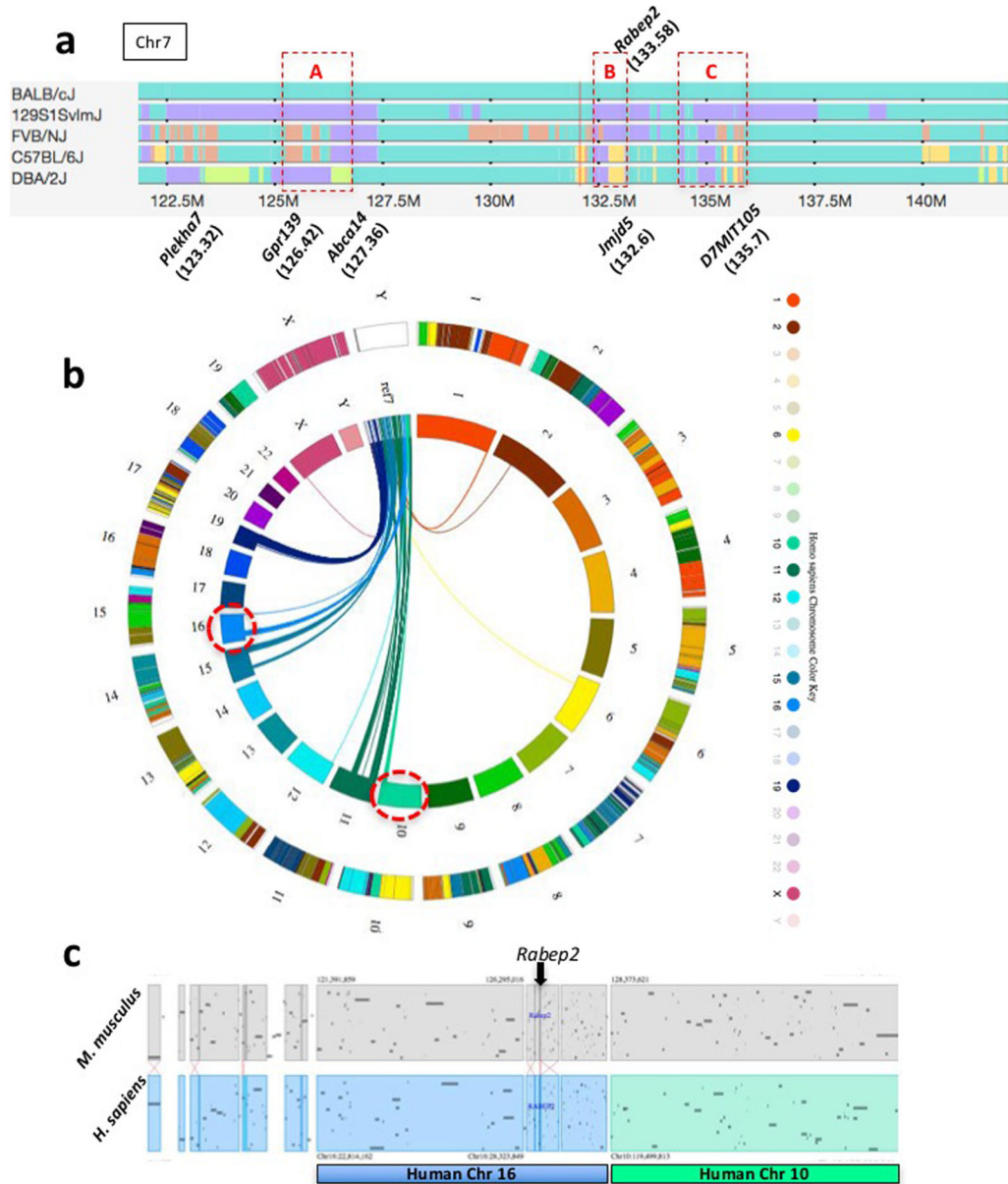
Figure 2: Haplotype blocks differing between BALB/cMed and strains that do not develop mammary tumors.

a) BALB/cJ haplotype blocks compared with 129S1SvimJ, FVB/NJ, C57BL/6J and

DBA/2J. BALB/c is assigned a single color (■) and subsequent strains are assigned the same color where their haplotypes match the first strain i.e. 129S1SvimJ alleles that differed from

BALB/c (■), FVB/NJ alleles different from BALB/cJ and FVB/NJ (■), C57BL/6 that

different from 3 previous tracks (■) and DBA2/J alleles that is different from all 4 track

above (■). Region A (125-127 Mb) defines a block that is within the shoulder region of linkage bounded by polymorphisms in *Plekha7* and *Abca14* in Fig. 1a. Regions B (132-133.2 Mb) and C (134.5-136 Mb) lie within the peak linkage and flank *Rabep2*. b) Map of human chromosomes syntenic with mouse chromosome 7. The Synteny Browser

was used to define relationships between mouse and human chromosomes [54]. The outer ring represents mouse chromsomes, the inner ring represents human chromsomes and the connections show syntenic regions to mouse chromosome 7. Regions of synteny to *Suprmam1* interval shown with red circle in the human chromosome 10 and 16. The color key represents human chromsomes with the non-syntenic chromosomes shaded. c) Expaned view of *Suprmam1* syntenic regions. The peak linkage surrounding the polymorphism in *Rabep2* is syntenic with human chromosome 16. The more telomeric region of the *Suprmam1* interval is syntenic with human chromosome 10. Grey bars indicate locations of genes.
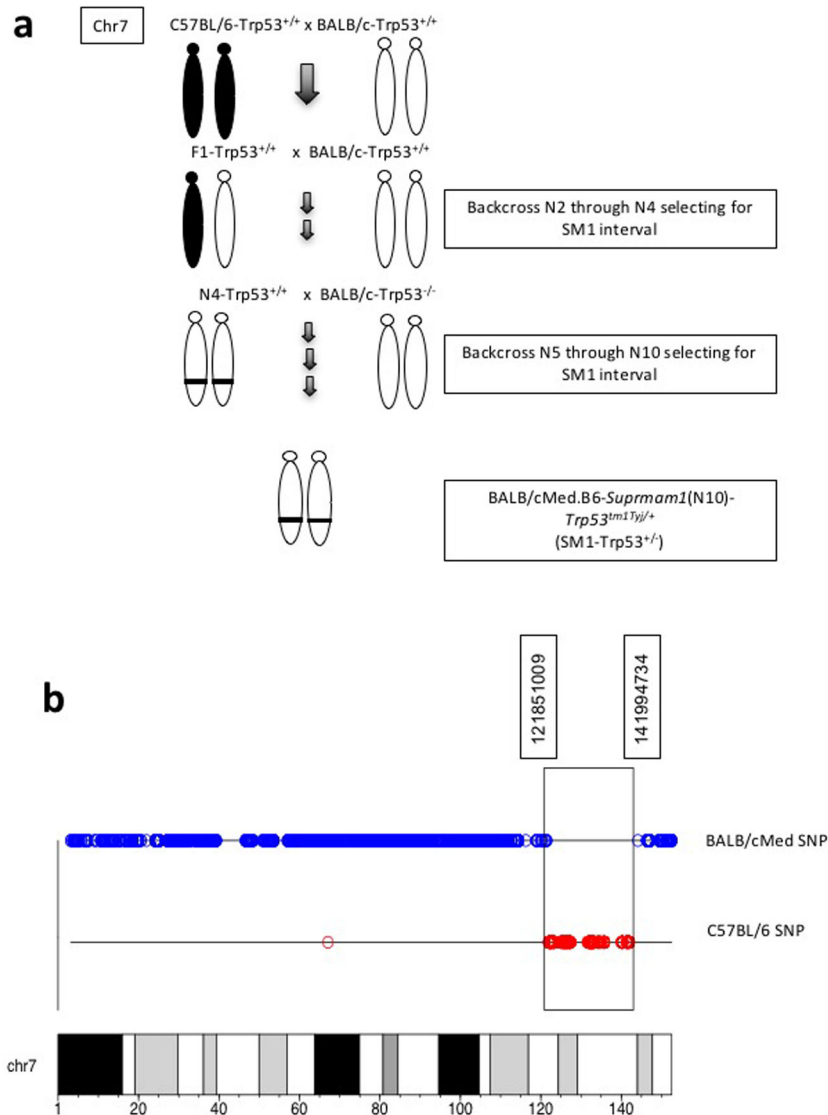
Figure 3: Generation and validation of BALB/cMed.B6-*SuprMam1*(N10)-*Trp53*^{tm1Tyj}/+ (SM1-*Trp53*^{+/−}) strain

a) Generation of the SM1 strain with marker assisted back-crossing. b) Mapping of SM1 congenic mouse chr7 with Affymetrix mouse diversity genotyping array. The blue circles represent BALB/cMed alleles and red circles represent C57BL/6J alleles. The SNPs shared between the strains have been removed for clarity. The region of chr7 having C57BL/6J alleles are highlighted in the box.
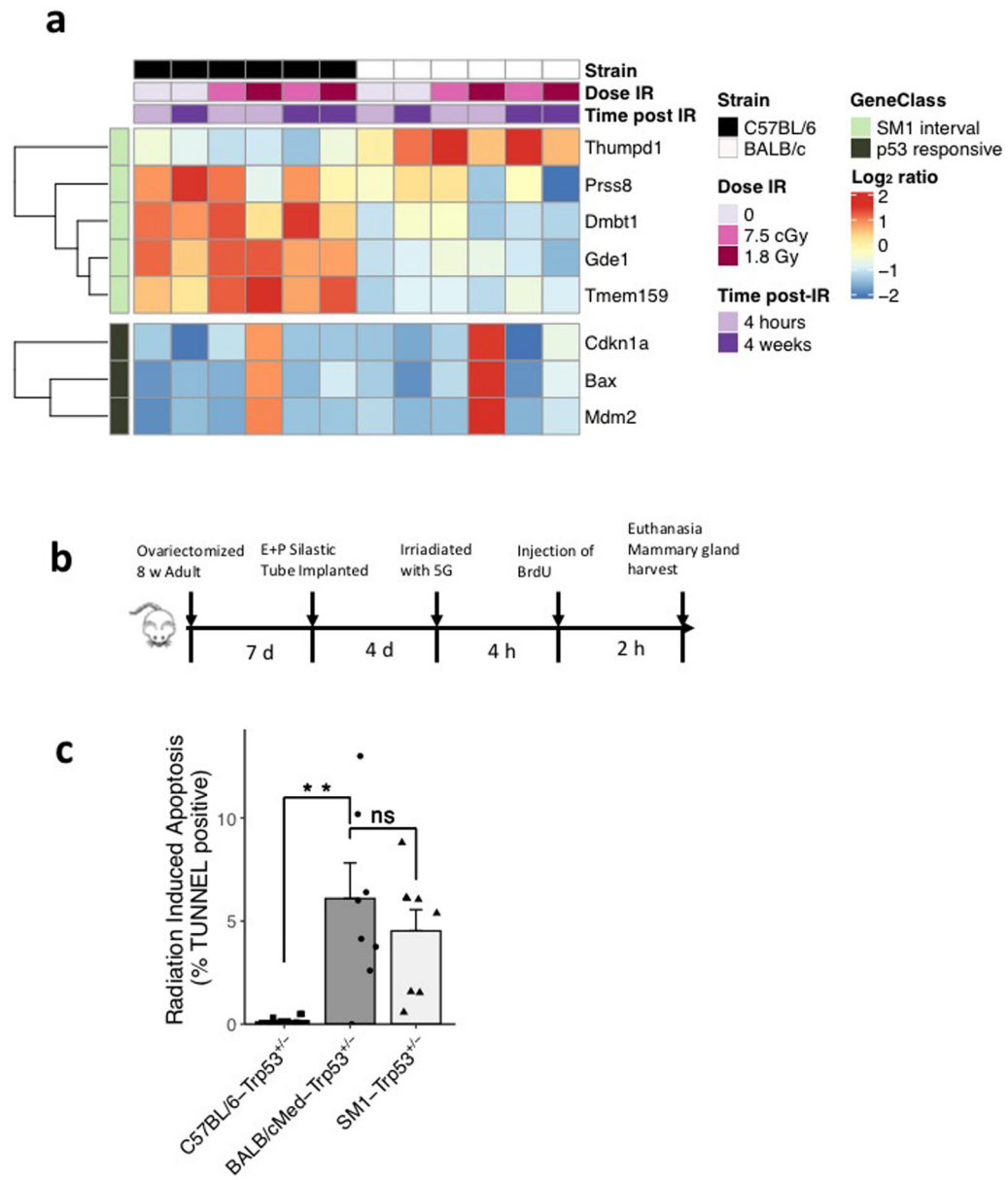
Figure 4: Variation to radiation sensitivity between strains.

a) Differential expression of genes within the *Suprmam1* interval in BALB/cJ and C57BL/6J mammary tissues. Expression of genes within *Suprmam1* were compared for differences due to doses of (0, 4x-1.8Gy, 4x-0.75Gy) and times post-irradiation (4h, 4wks). Expression of genes within the *Suprmam1* interval (upper panel) show strain-specific patterns (log2 FC >1.5 in 3 or more conditions). Selected radiation-responsive genes that are p53-dependent are included for comparison (lower panel). b) Experimental procedure for TUNEL assay in mouse mammary gland. c) Quantification of TUNEL positive cells. C57BL/6-*Trp53*$^{+/-}$ (n = 8) mammary glands show very few TUNEL positive cells, BALB/cMed-*Trp53*$^{+/-}$ (n = 7) and SM1-*Trp53*$^{+/-}$ (n = 4) mammary glands exhibited high TUNEL positivity. ** $p < 0.01$.
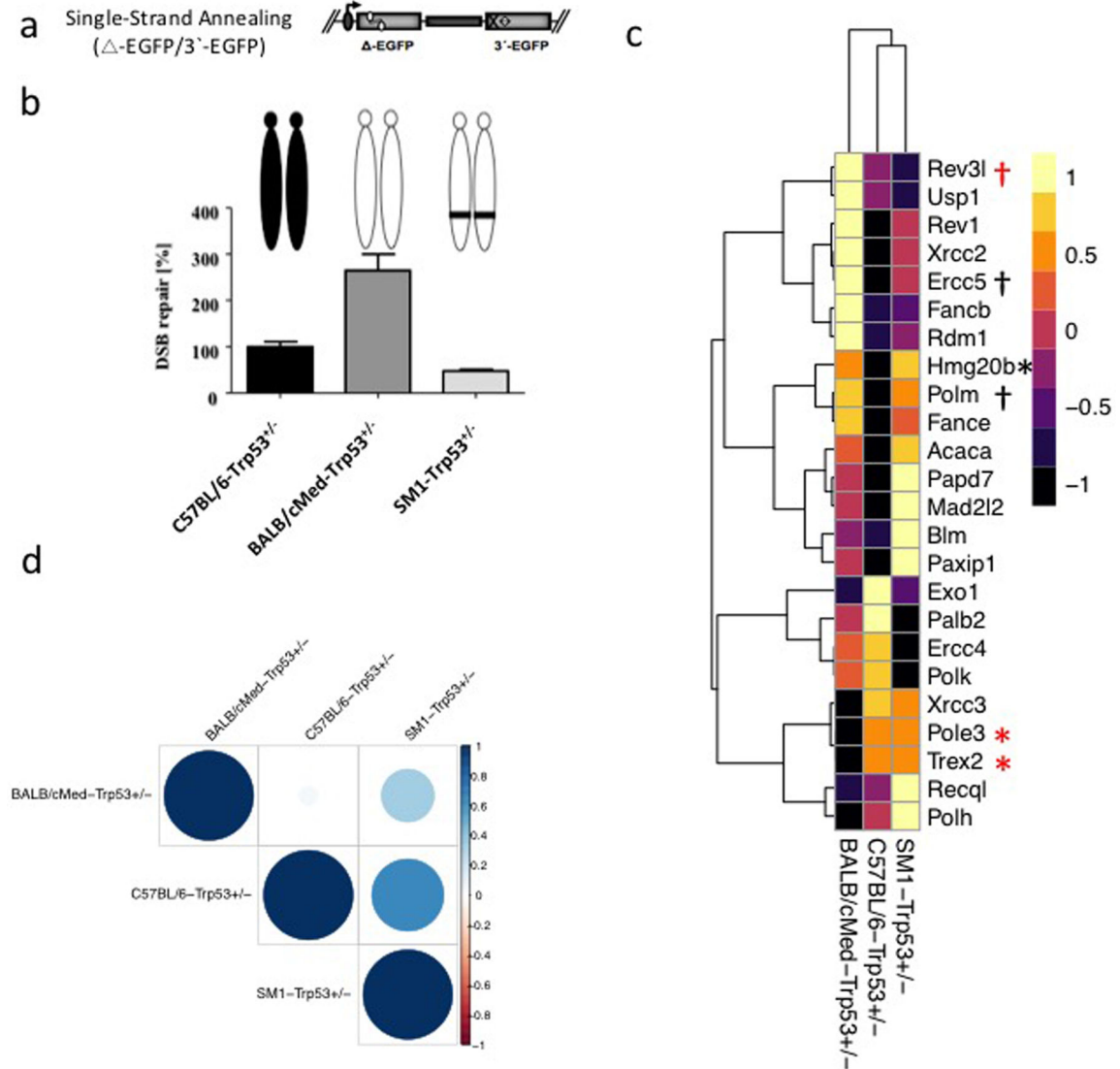
Figure 5: Single-strand annealing and gene expression differences between C57BL/6-*Trp53*$^{+/-}$, SM1-*Trp53*$^{+/-}$ and BALB/c-*Trp53*$^{+/-}$ MEFs

a) The SSA reporter construct. The construct ΔEGFP-3'-EGFP carries an acceptor EGFP gene variant, in which 46 bp encompassing the chromophore codons are replaced by an I-SecI recognition site (ΔEGFP) and a 5'-truncated EGFP donor gene (3´-EGFP). b) SSA repair efficiency in MEFs. C57BL/6J-*Trp*53$^{+/-}$ executed significantly less repair compared to BALB/cMed-*Trp*$^{+/-}$ whereas SM1-*Trp53*$^{+/-}$ showed comparative repair efficiency. *** *p* < 0.001 . c) Heatmap showing similarity of DNA repair gene expression profiles of MEFs from three strains . *p* < 0.05 compares † across all strains, † BALB/cMed-*Trp53*$^{+/-}$ and C57BL/6J-*Trp53*$^{+/- -}$, * C57BL/6J-*Trp53*$^{+/-}$ and SM1-*Trp53*$^{+/-}$ and * BALB/cMed-*Trp53*$^{+/-}$ with both SM1-*Trp53*$^{+/-}$ or C57BL/6-*Trp53*$^{+/-}$. d) Similarity of DNA repair gene expression pattern between SM1-*Trp53*$^{+/-}$ and C57BL/6-*Trp53*$^{+/-}$. Spearman's rank-ordered correlation analysis of qRT-PCR expression data on 24 genes from three strains show that DNA repair gene expression of SM1-*Trp53*$^{+/-}$ is strongly correlated with C57BL/6-*Trp53*$^{+/-}$ but not with BALB/c-*Trp53*$^{+/-}$.
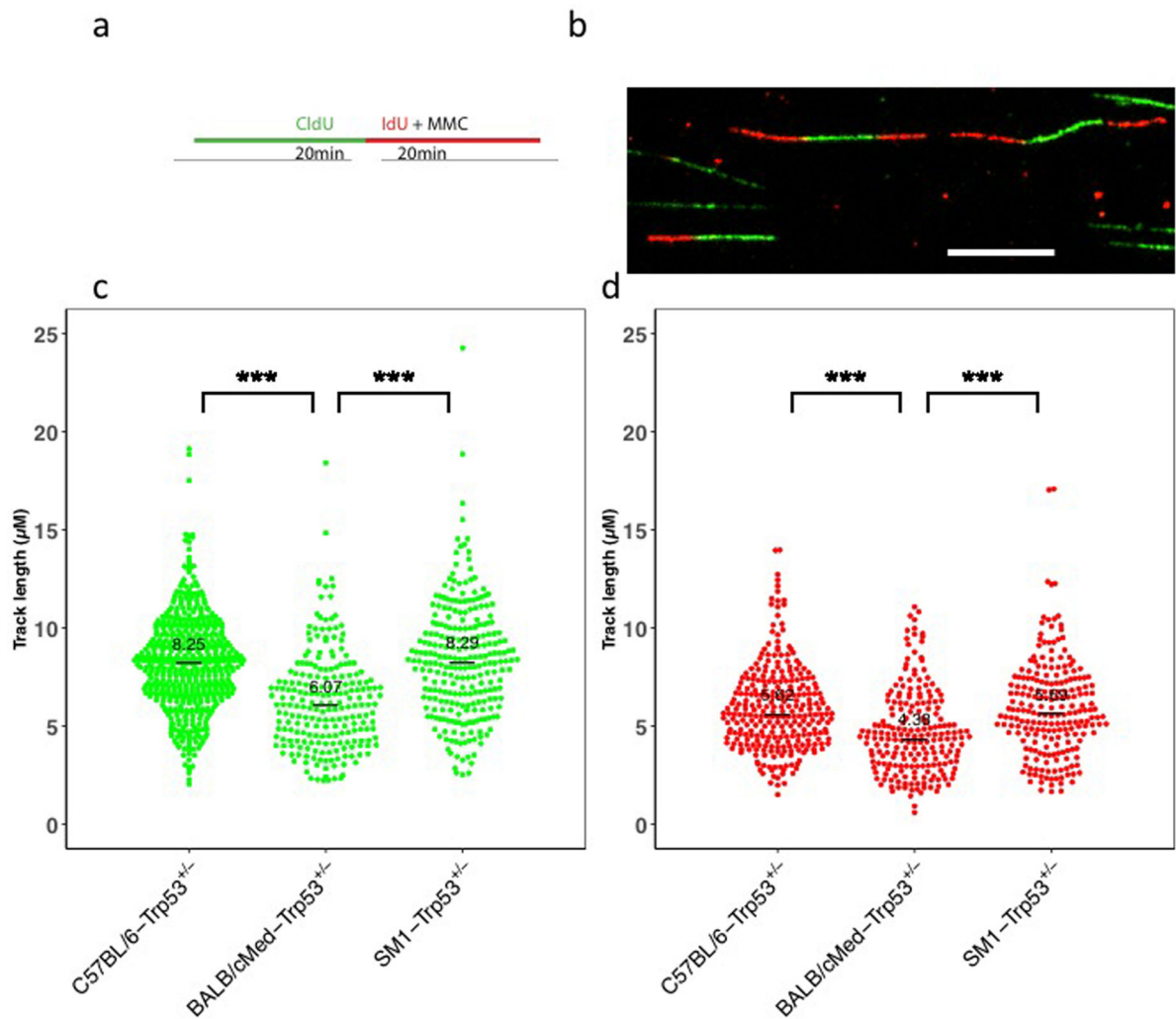
Figure 6: Difference in replication fork processivity between C57BL/6-*Trp53*^{+/−}, SM1-*Trp53*^{+/−} and BALB/c-*Trp53*^{+/−} MEFs

a) Replication forks of DNA synthesized by MEFs from C57BL/6J-*Trp53*^{+/−}, BALB/cMed-*Trp53*^{+/−} and SM1-*Trp53*^{+/−} during 20min pulse label with Cldu (Green) and Idu and MMC (Red). b) Representative image of the replication-fork used for measuring fork-length c) Replication-fork length is longer in C57BL/6J-*Trp53*^{+/−} MEFs compared to BALB/cMed-*Trp53*^{+/−} and comparable to SM1-*Trp53*^{+/−}. d) Replication-fork length in the presence of MMC is also longer in C57BL/6J-*Trp53*^{+/−} MEFs compared to BALB/cMed-*Trp53*^{+/−} and the fork-length is rescued in the SM1-Trp53^{+/−} MEFs. *** $p < 0.001$. Scale bar = 10μM

Table 1:

Positions of the SNP/markers used in the linkage analysis of mammary tumor phenotypes in female [(C57BL/6 x BALB/c) x BALB/c]-N2-*Trp53*$^{+/-}$ mice in reference genome NCBIM37 (mm10).

The physical positions of markers are indicated by the midpoint between the sequence start and end to accommodate length polymorphisms.

Markers/SNP	Gene/Markers	Chr	Mid (in MB)
rs3023136	Aldh1a3, Asb7	7	73.58
rs3023148	Dlgh2	7	98.30
D7MIT96	D7MIT96	7	107.65
rs16789781	Nlrp14	7	114.33
D7MIT281	D7MIT281	7	119.36
rs3023153	Rras2	7	121.22
rs3023157	Sox6	7	122.48
rs32285976	Plekha7	7	123.32
rs3023159	Gpr139, Gp2	7	126.43
rs32610298	Abca14	7	127.36
D7MIT68	D7MIT68	7	132.49
rs32988178	Jmjd5	7	132.60
rs3023166	Il4ra,Il21r	7	132.72
Il21	Il21	7	132.77
rs33080487	Rabep2	7	133.58
D7MIT105	D7MIT105	7	135.71
rs32420445	Dock1	7	141.98

Table 2:
Candidate genes within Suprmam1 interval.

Genes were identified based on 1) GO term 2) having coding non-synonymous SNP variation 3) having orthologous causal variant to breast neoplasm.

	Mouse Gene	NCBIm37 Position	Synteny Block	Human Gene	GRCh37 Positions	Selection Method
1	Nupr1	7:133766763-133770524(−1)	-	NUPR1	16:28550495-28550495(−1)	GO Term: DNA Damage
2	Mapk3	7:133903115-133909333(1)	-	MAPK3	16:30134827-30134827(−1)	
3	D7Ertd443e	7:141457945-141577344(−1)	-	C10orf90	10:128359079-128359079(−1)	
4	Plk1	7:129302951-129313389(1)	-	PLK1	16:23701688-23701688(1)	
5	Taok2	7:134009192-134028217(−1)	-	TAOK2	16:30003582-30003582(1)	
6	Nsmce1	7:132611154-132635110(−1)	B	NSMCE1	16:27280115-27280115(−1)	
7	Nsmce4a	7:137676037-137716632(−1)	-	NSMCE4A	10:123734732-123734732(−1)	
8	Kif22	7:134171246-134185934(−1)	-	KIF22	16:29816706-29816706(1)	GO Term: DNA Repair
9	Slx1b	7:133832982-133839298(−1)	-	SLX1B	16:29469540-29469540(1)	
10	Bccip	7:140901016-140912828(1)	-	BCCIP	10:127542264-127542264(1)	
11	Smg1	7:125274832-125387151(−1)	A	SMG1	16:18816175-18937776(−1)	
12	Mcmbp	7:135839955-135884009(−1)	C	MCMBP	10:121652068-121652068(−1)	GO Term: DNA Replication
13	Kctd13	7:134072393-134089145(1)	-	KCTD13	16:29938356-29938356(−1)	
14	Palb2	7:129250776-129276460(−1)	-	PALB2	16:23652631-23652631(−1)	GO Term: Homologous Recombination
15	Ppp4c	7:133929421-133935985(−1)	-	PPP4C	16:30096698-30096698(1)	
16	Fgfr2	7:137305965-140315033(−1)	-	FGFR2	10:123237848-123357972(−1)	Variant associated with PhenGenI phenotype: breast neoplasm
17	Ate1	7:137535040-137663475(−1)	-	ATE1	10:123499939-123688316(−1)	
18	Syt17	7:125525370-125587066(−1)	A	SYT17	16:19179293-19279652(1)	
19	6330503K22Rik	7:125856066-125880538(1)	A	CCP110	16:19535133-19564730(1)	MDA (Coding nonsynonymous)
20	Il21r	7:132746943-132777084(1)	B	IL21R	16:27413483-27462115(1)	
21	Dnahc3	7:127066231-127238691(−1)	-	DNAH3	16:20943804-21170762(−1)	
22	Tgfb1i1	7:135390326-135398287(1)	C	TGFB1I1	16:31482906-31489281(1)	SNP Viewer (Stop gained/lost)
23	Itgal	7:134439774-134478651(1)	-	ITGAL	16:30483979-30534289(1)	